Opportunity of Negative Capacitance Behavior in Ferroelectrics for High-Density and Energy-Efficient Flash-type In-Memory Computing Applications

Prof. Sanghun Jeon

School of Electrical Engineering, KAIST

Outline

1. Introduction

Theoretical Model of NC in DE/FE Bi-Layer

❖ Basic Concept of NC in DE/FE Bi-Layer

- **Ferroelectrics has a W shape in U versus P curve showing negative capacitance region**
- **To stabilize negative capacitance behavior, ferroelectric should have heterostructure with dielectric, now it becomes stable**

FE single-layer　　DE single-layer　　DE/FE bi-layer

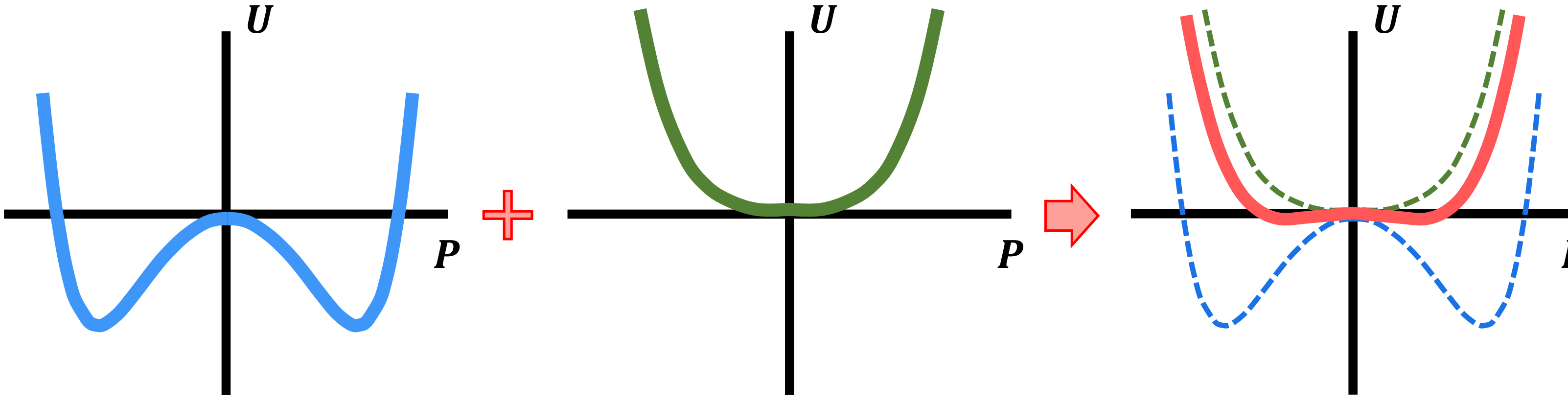

$U = \alpha P_S^2 + \beta P_S^2 + \gamma P_S^2 - EP_S$

$U = \frac{Q^2}{2C}$

NC with no hysteresis

2. HfO_2 based Ferroelectric Thin Films

Difference Between MFM and MFIM Systems

❖ Charging capacitor in MFM and MFIM systems

- For MFM capacitor, the polarization of ferroelectric is perfectly compensated by free carrier of the electrode

MFM System

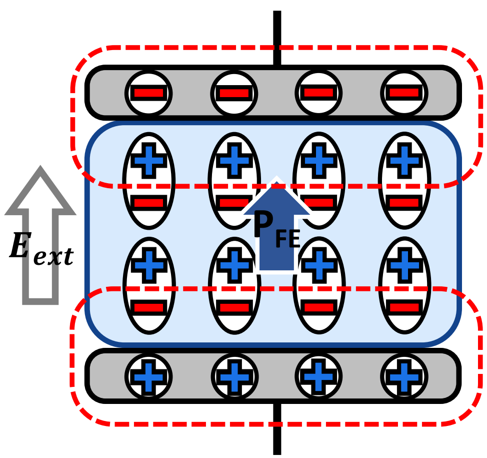

MFIM System

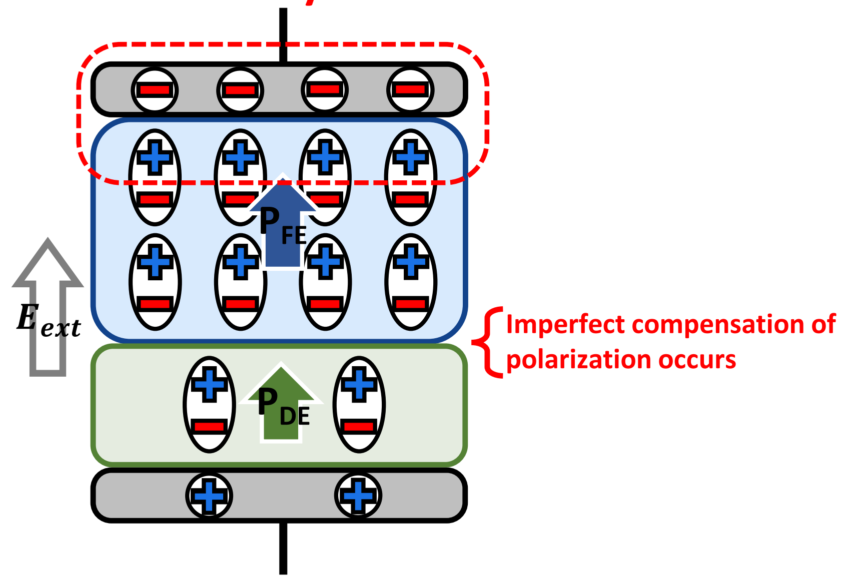

Difference Between MFM and MFIM Systems

❖ E_{dep} generation due to incomplete compensation of FE polarization

- **In MFIM system, the charge screening of the polarization is imperfect at the interface between ferroelectric and dielectric materials, generating the internal field.**
- **Therefore, there is a finite depolarization field (E_{dep}) inside of the FE layer.**

MFM System

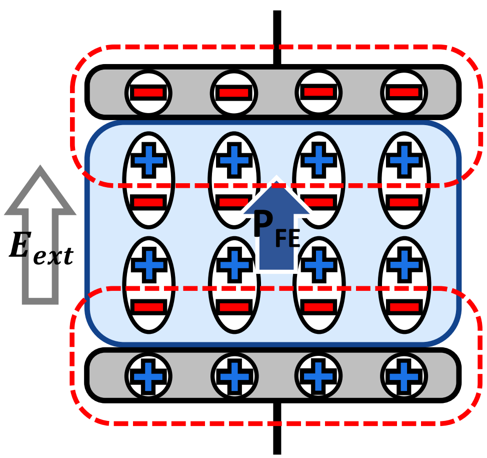

MFIM System

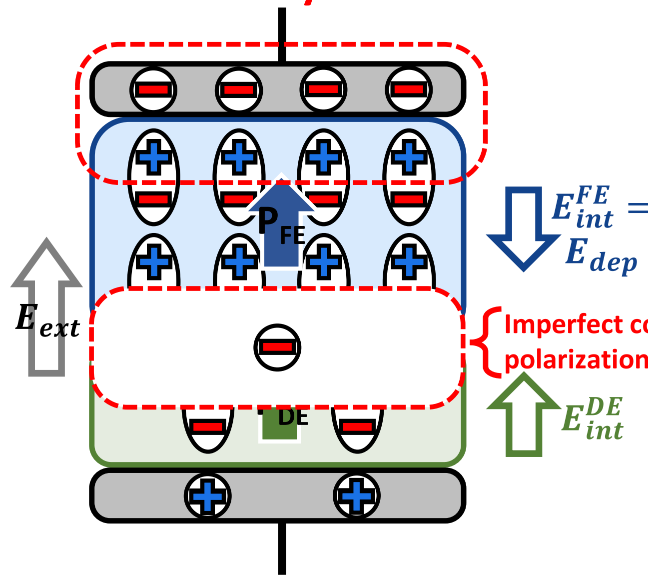

$$U_S = \alpha P_S^2 + \beta P_S^4 + \gamma P_S^6 - E_{ext} P_S$$

$$U_S = \alpha P_S^2 + \beta P_S^4 + \gamma P_S^6 - \left[E_{ext} \cdot P_s + \frac{\sigma_i \cdot P_s - \frac{1}{2} {P_s}^2}{\varepsilon_0 \cdot l_{FE}} \cdot \left(\frac{\varepsilon_{DE}}{l_{DE}} + \frac{\varepsilon_{FE}}{l_{FE}} \right)^{-1} \right]$$

Reversible Single-Domain Ferroelectric (RSFE)

Materials science

❖ **To stabilize and utilize the NC effect, we need to develop a homogeneously aligned FE phase, such as a single-domain**

- **In the multi-domain system, the E_{dep} inside the FE layer is significantly reduced compared to the single-domain case.**
- **According to the domain switching mechanism, in the absence of a driving force that re-establishes the initial domain state, the NC effect caused by domain switching becomes irrecoverable or a one-time phenomena.**

Single-domain

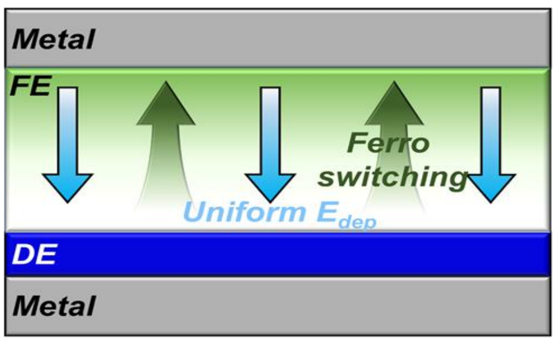

$$\varepsilon_0 \varepsilon_{DE} E_{DE} = \varepsilon_0 \varepsilon_{FE} E_{FE} + P_S$$

Multi-domain

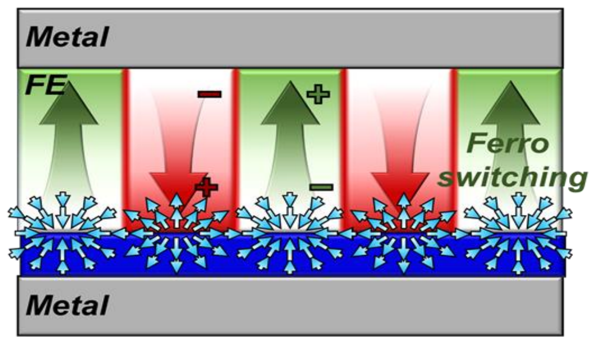

$$\varepsilon_0 \nabla^2 \varphi = \vec{\nabla} \cdot \vec{P}$$

※ φ : electric potential
$\vec{\nabla} \cdot \vec{P}$: space charge

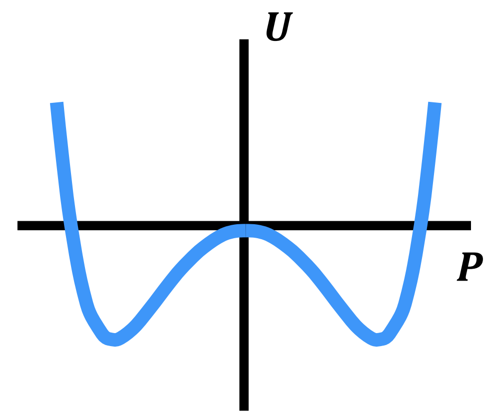

$$U = \alpha P_S^2 + \beta P_S^2 + \gamma P_S^2 - EP_S$$

How to Make an Reversible Single Domain Ferroelectric Film?

Process

❖ High Pressure Post Deposition Annealing (HPPDA)

- **To form a CMOS-compatible RSFE-HZO films, HPPDA at 200 atm. were performed in a forming gas (the mixture of 4% H_2 and 96% N_2).**
- **FG-HPPDA enables to form a homogeneously aligned domain phase and reversible domain switching via a strain gradient induced internal field and chemically induced surface polarization pinning.**

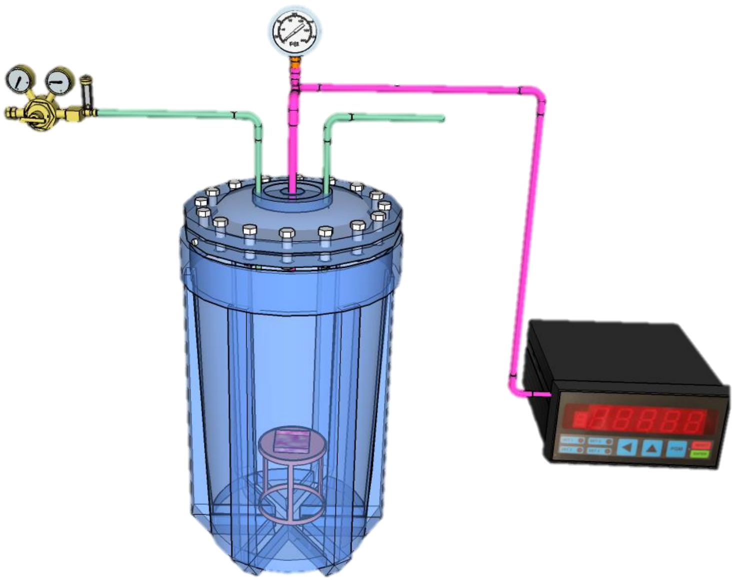

HPA Equipment

- **Pressure : 1~200atm.**
- **Gas : N_2, FG(H_2 4%, N_2 96%)**
- **Temperature : ~ 600℃**

Flexoelectric Effect

❖ Ferroelectric characteristics can be tuned by the flexoelectricity

- **The flexoelectric effect describes an electric field that is generated by a strain gradient.**
- **$E_{Internal}$ can be large enough that a single-domain forms.**

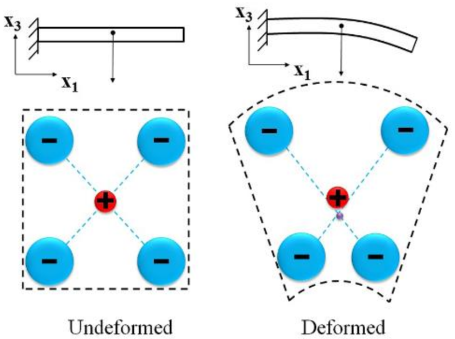

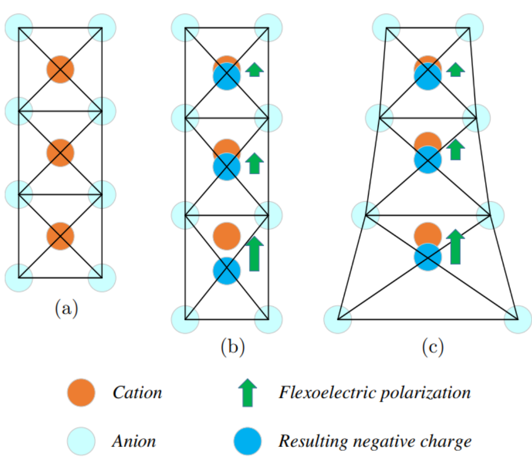

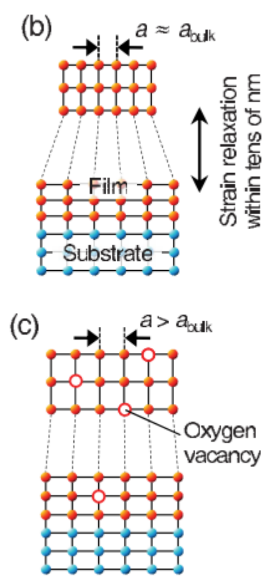

$$E_{Internal} = \frac{e}{4\pi\varepsilon_0 a}\frac{\partial u}{\partial z}$$

$\frac{\partial u}{\partial z}$: strain gradient

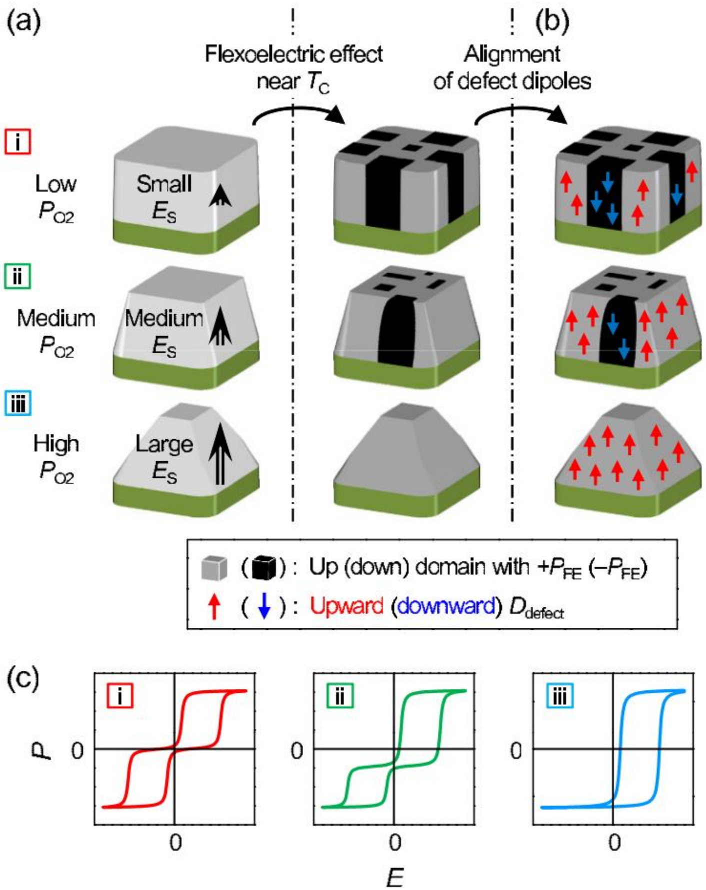

Flexoelectric Effect in HfO_2 Ferroelectric Films

❖ Ferroelectric characteristics can be tuned by the flexoelectricity

- The flexoelectric effect describes an electric field that is generated by a strain gradient.
- $E_{Internal}$ can be large enough that a single-domain forms.

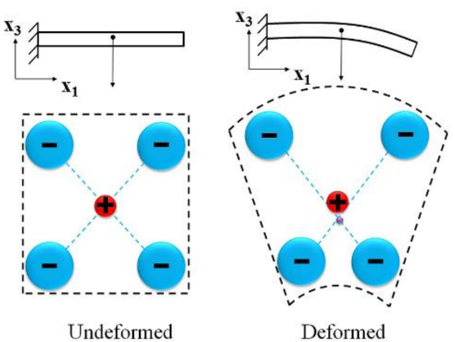

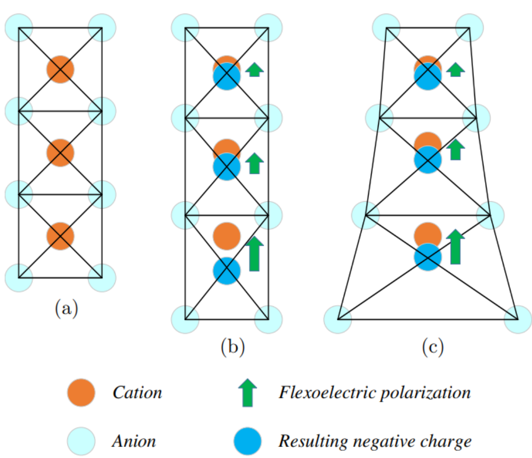

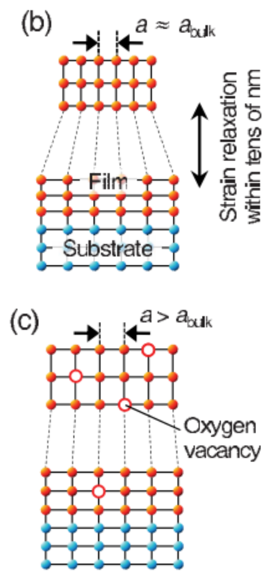

$$E_{Internal} = \frac{e}{4\pi\varepsilon_0 a}\frac{\partial u}{\partial z}$$

$\frac{\partial u}{\partial z}$: strain gradient

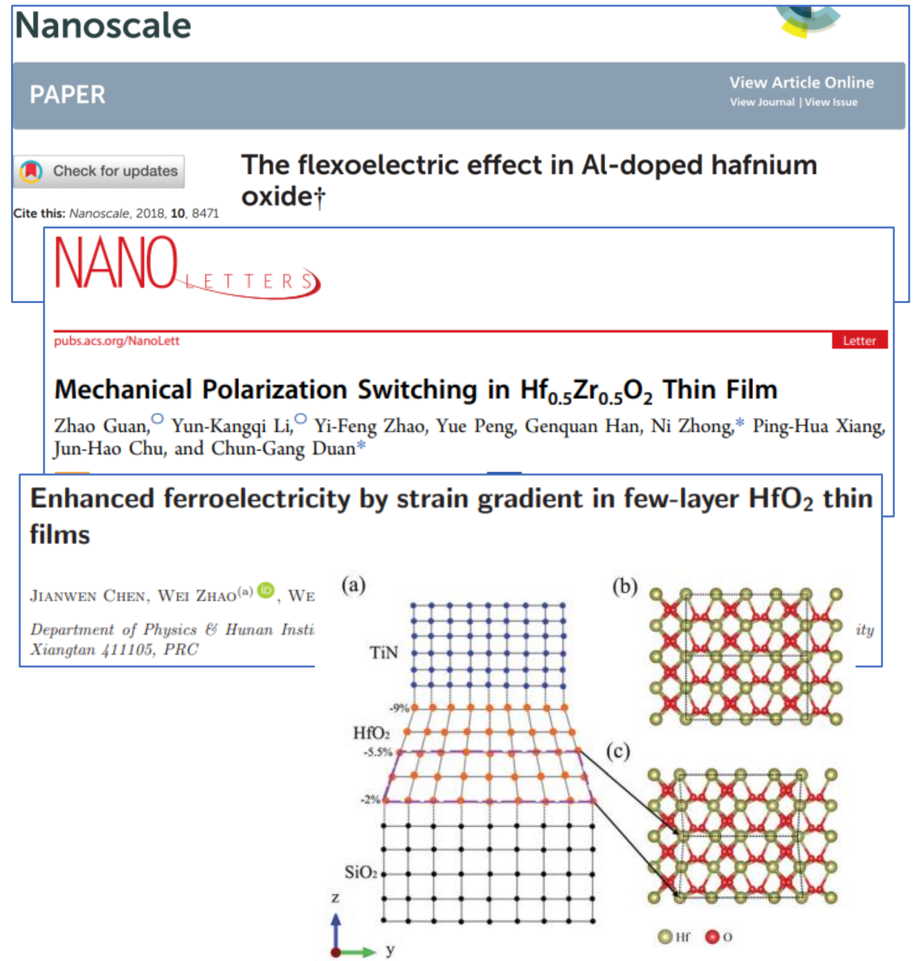
Nanoscale

PAPER

View Article Online
View Journal | View Issue

Check for updates

Cite this: Nanoscale, 2018, 10, 8471

The flexoelectric effect in Al-doped hafnium oxide†

NANO LETTERS

pubs.acs.org/NanoLett

Letter

Mechanical Polarization Switching in $Hf_{0.5}Zr_{0.5}O_2$ Thin Film

Zhao Guan, Yun-Kangqi Li, Yi-Feng Zhao, Yue Peng, Genquan Han, Ni Zhong,* Ping-Hua Xiang, Jun-Hao Chu, and Chun-Gang Duan*

Enhanced ferroelectricity by strain gradient in few-layer HfO_2 thin films

Jianwen Chen, Wei Zhao[a], We

Department of Physics & Hunan Insti
Xiangtan 411105, PRC

Flexoelectric Effect of HPPDA

❖ Estimation of Strain and Strain Gradient for Hafnia by HP PDA

- GIXRD is a powerful tool for determining the depth profile of the in-plane lattice consta
- While the lattice constant averaged over the entire film region can be measured with a large λ_i, we obtained information on the value of a near the film surface with a small λ_i.

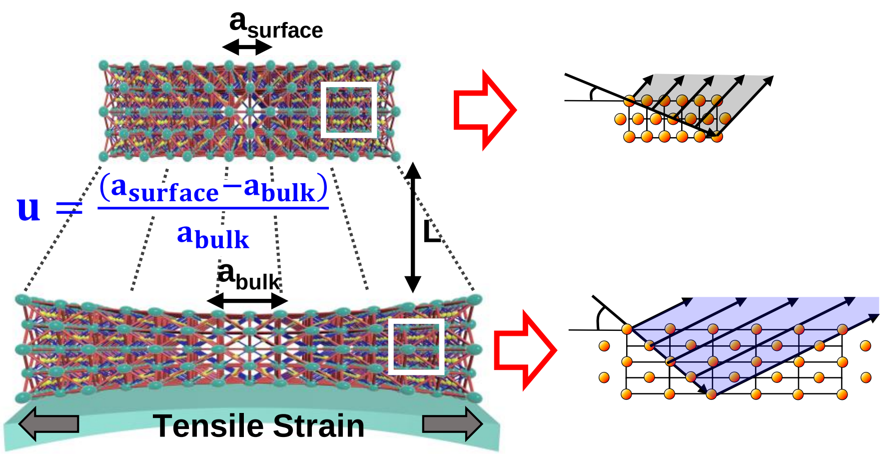

$$u = \frac{(a_{surface} - a_{bulk})}{a_{bulk}}$$

❖ Thermal Expansion Coefficient [10^{-6}/°C]

W	Mo	Pt	TiN	Ni
4.5	5	8~9	9.4	13

Six-circle high-resolution GIXRD (HR-GIXRD)

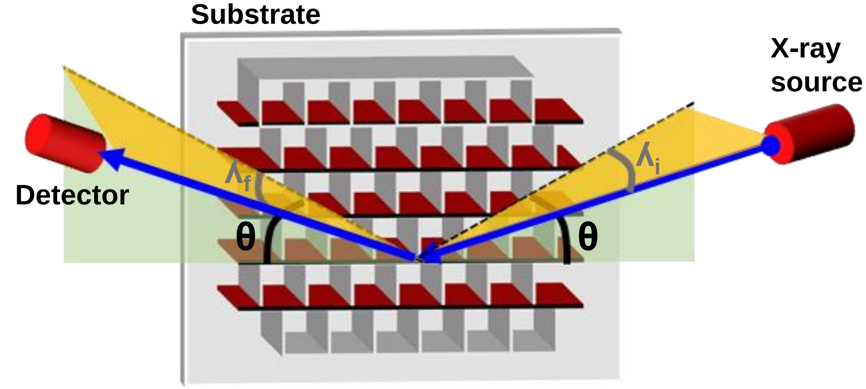

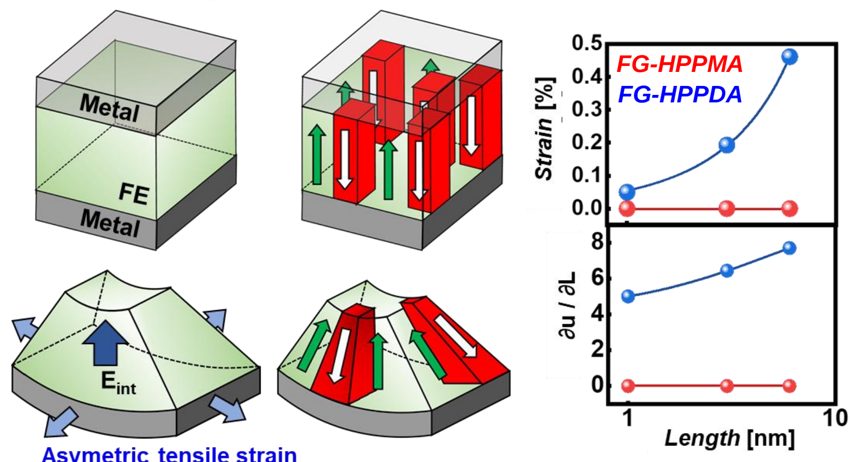

Surface Effect of FG-HPPDA

❖ Chemically Induced Surface Polarization Pinning

- When H_2 molecules are adsorbed on the HZO surface, the surface becomes extensively hydroxylated, which enhances H_2-induced vacancy formation.
- The surface hydroxyl groups (OH^-) can align the polarization direction in the upward direction.

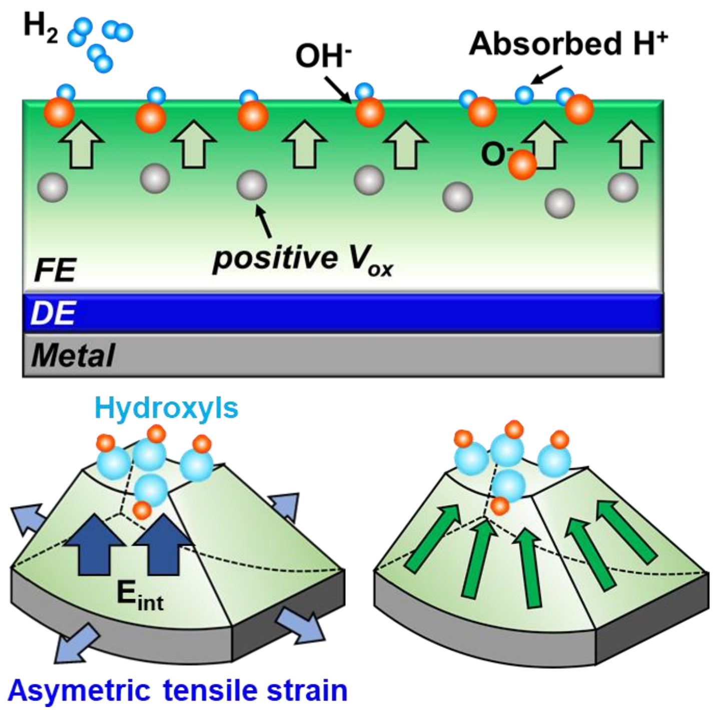

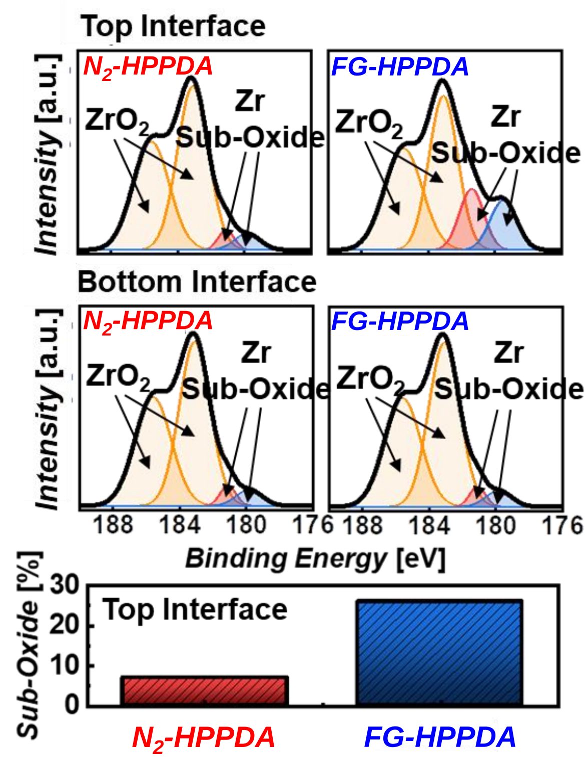

Source: H. Lee, Nano Lett. (2016)

Summary of FG-HPPDA Effects

❖ **FG-HPPDA plays a significant role in defining the domain configurations**

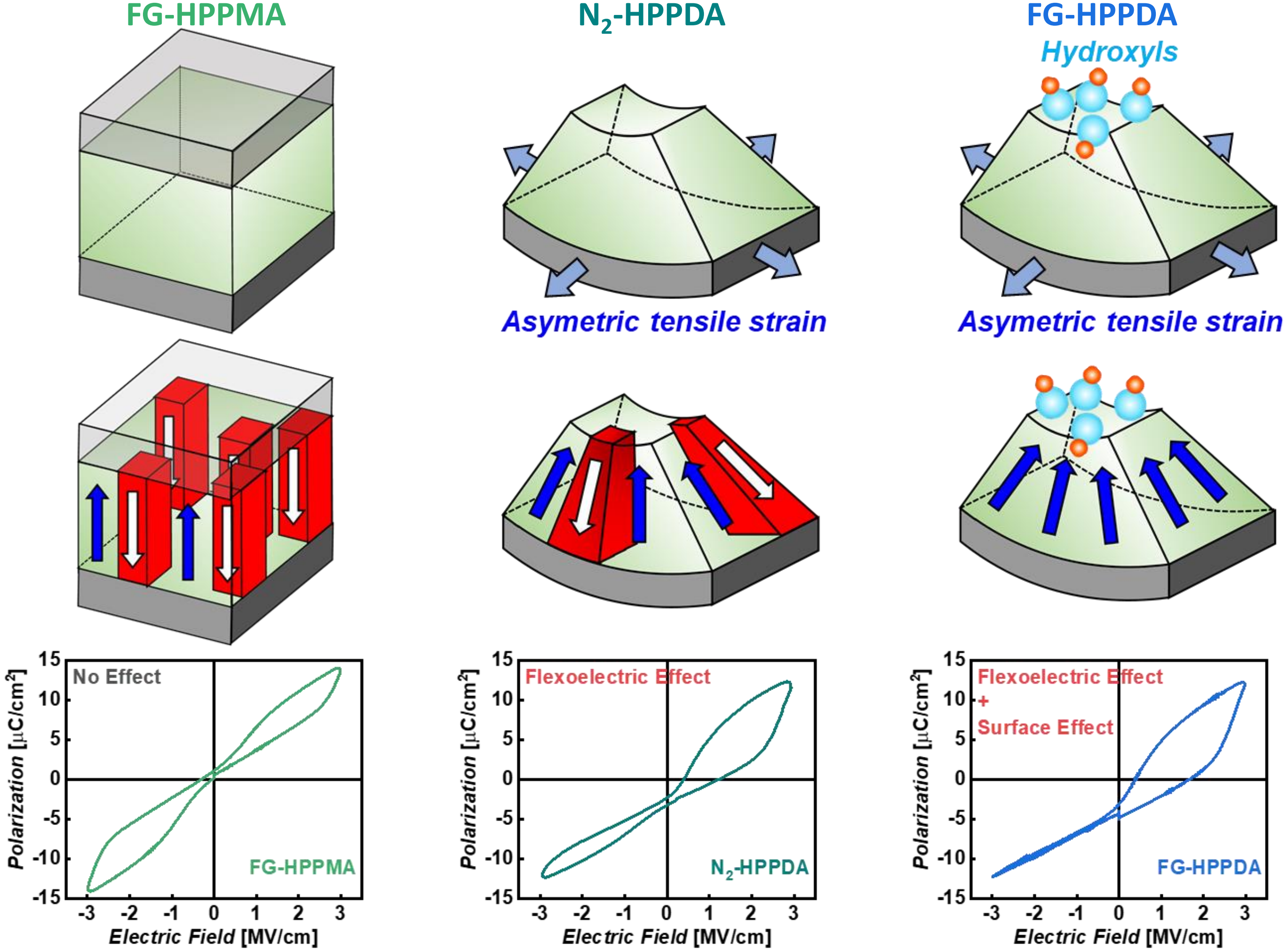

3. Transient NC Effect in RSFE-HZO/AlO Bilayer

Landau Free Energy Diagrams of Bilayer

❖ **Energy diagram calculated by the landau theory equation of the bi-layer structure of HZO and AlO with various electrical characteristics.**

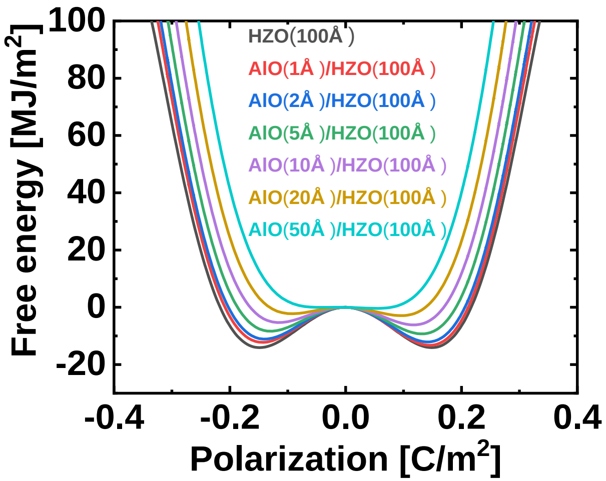

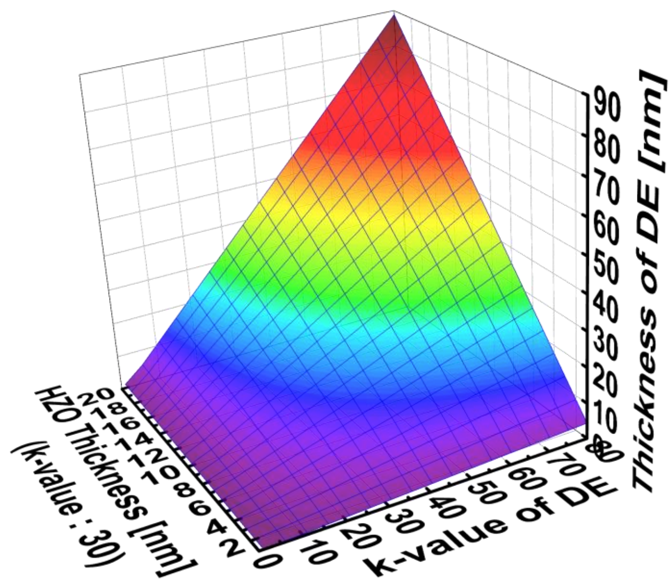

$$U_S = \alpha P_S^2 + \beta P_S^2 + \gamma P_S^2 - E_{ext} P_S - \int E(P, \sigma_i) dP$$

$$= \alpha P_S^2 + \beta P_S^2 + \gamma P_S^2 - \left[E_{ext} \cdot P_S + \frac{\sigma_i \cdot P_s - \frac{1}{2} {P_s}^2}{\varepsilon_0 \cdot l_{FE}} \cdot \left(\frac{\varepsilon_{DE}}{l_{DE}} + \frac{\varepsilon_{FE}}{l_{FE}} \right)^{-1} \right]$$

Electrical Characteristics of bilayer in Static Environment

❖ Bilayer with HZO & AlO films shows negligible hysteresis with lower capacitance density than the AlO layer suggesting that the two layers work as the normal dielectric layer.

RSFE-HZO Single-layer

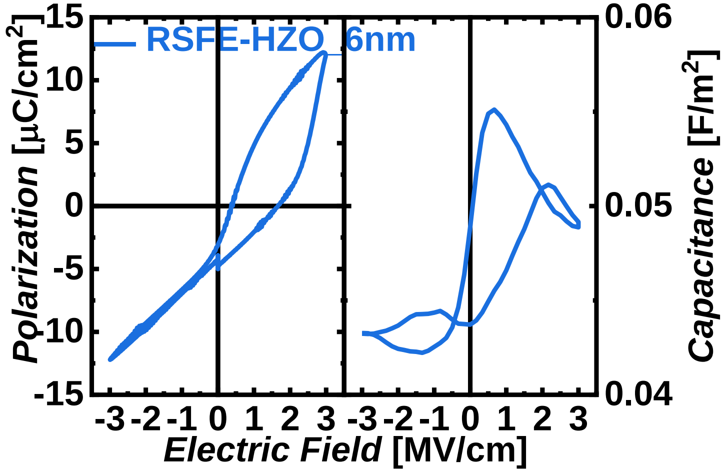

RSFE-HZO/AlO Bi-layer

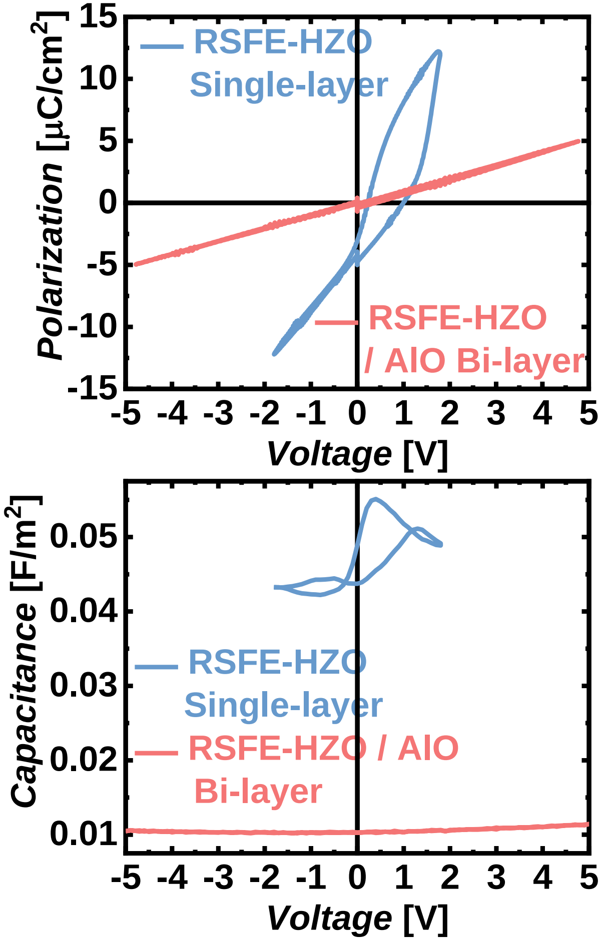

Pulse Type Switching Measurement Scheme

❖ **A short pulse type charge-voltage measurement**

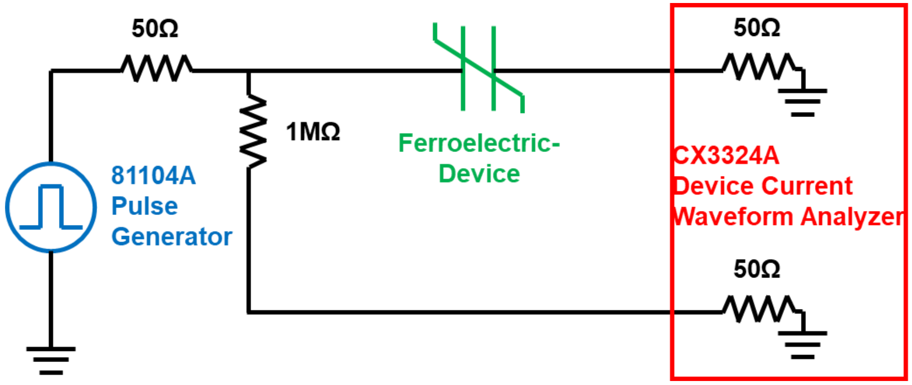

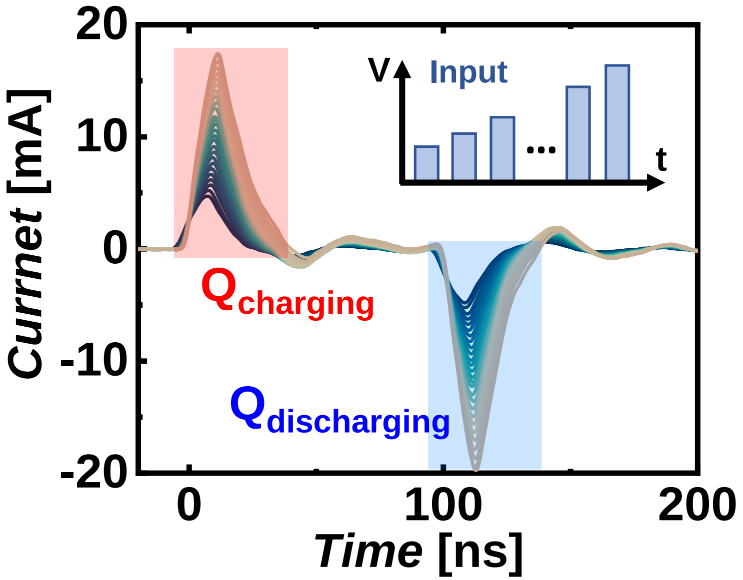

Electrical Characteristics of bilayer in Short Pulse Meas.

❖ **Charge Density vs. Voltage and Cap. vs Voltage for bilayer in DC and pulse type measurement**

DC

Pulse

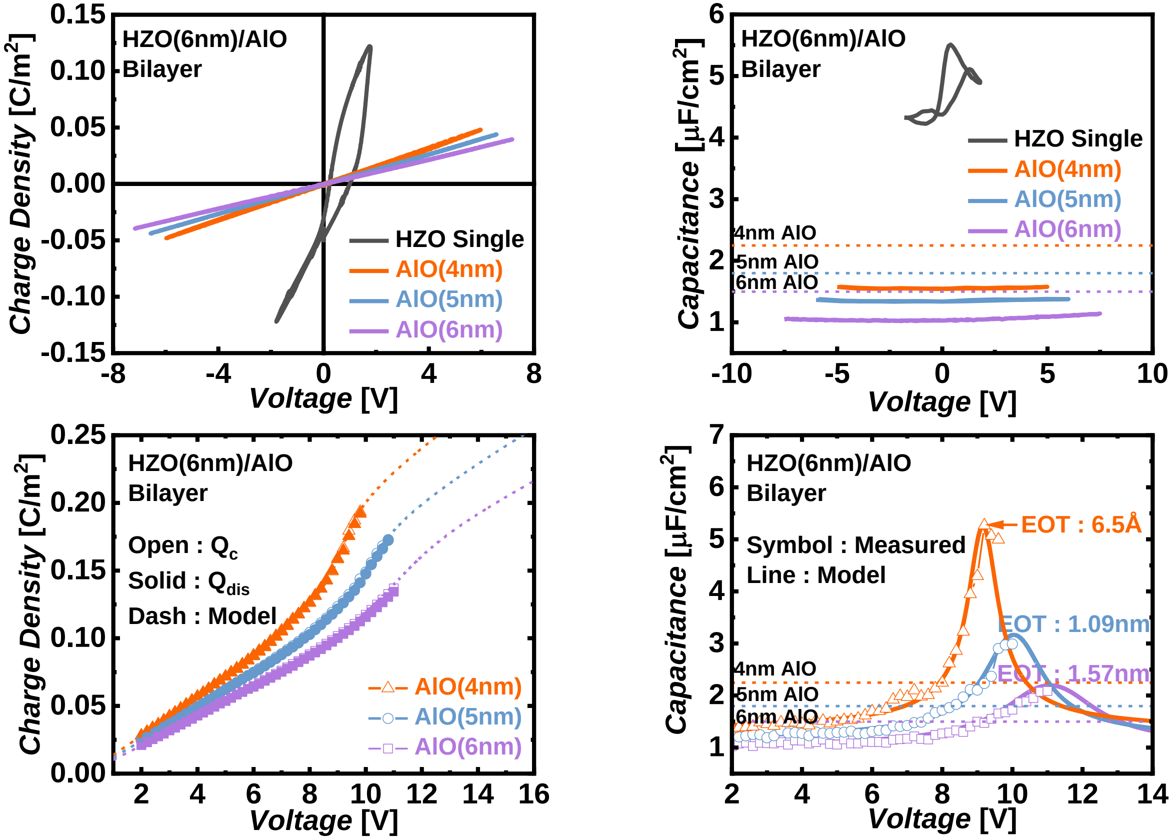

Landau-Ginzburg-Devonshire (LGD) Theory

❖ Fitted lines based on the LGD model is applied to the RSFE-HZO/AlO.

- **The high coincidence between theoretical model and experimental results indicates that such charge boosting effect must be ascribed to the reversible motion of the FE polarization in the RSFE-HZO layer.**

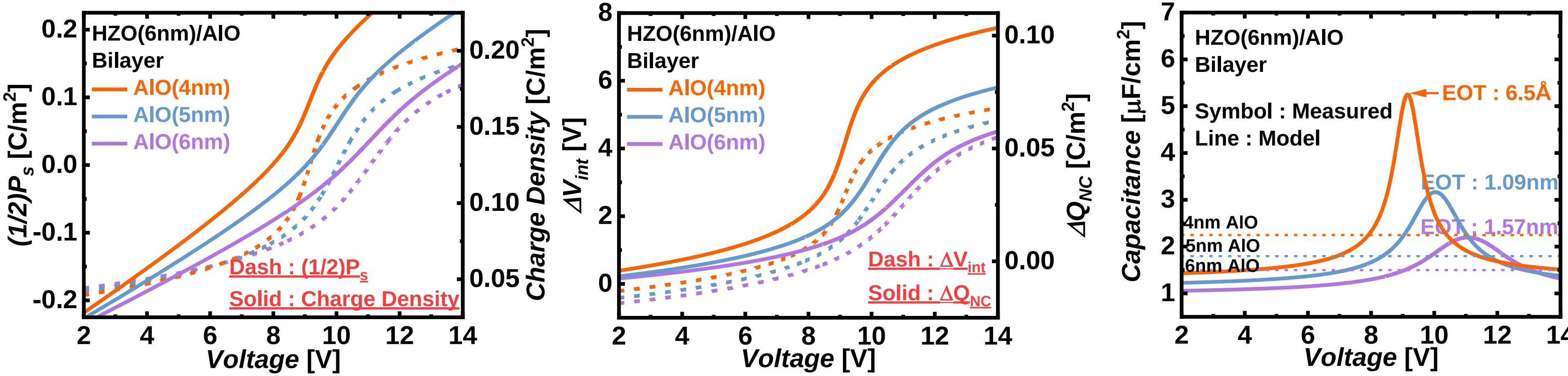

Ferroelectric	$H_{0.25}Z_{0.75}O_2$ / 6nm		
Dielectric	AlO / 6nm	AlO / 5nm	AlO / 4nm
$\alpha/\beta/\gamma$		-5.4E8 / 8.37E8 / 1.13E10	
δ		0.1	
σ_i [C m^{-2}]	-0.147	-0.16	-0.178
EOT	**1.57 nm**	**1.09 nm**	**6.5 Å**

4. Application : Charge Trap Flash Memory with NC- Effect Blocking Layer

Motivation

- ❖ Researchers have presented various works regarding high-performance CTF devices with functional blocking oxide.
- ❖ However, performance-improvement limitations still exist.

3D NAND Flash Structure

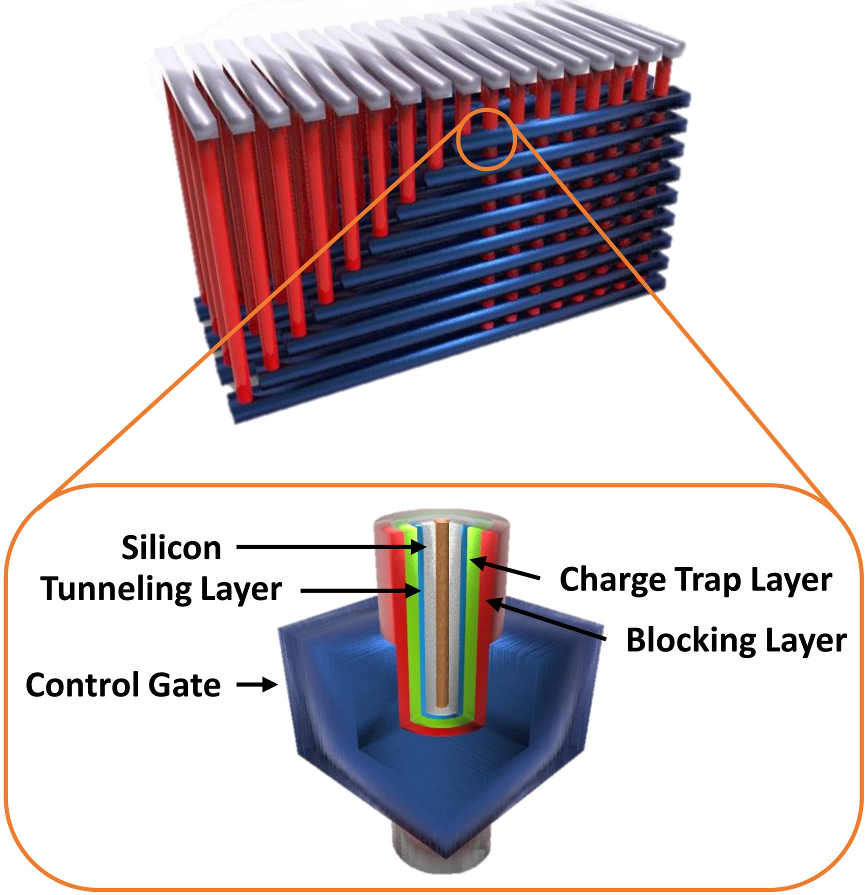

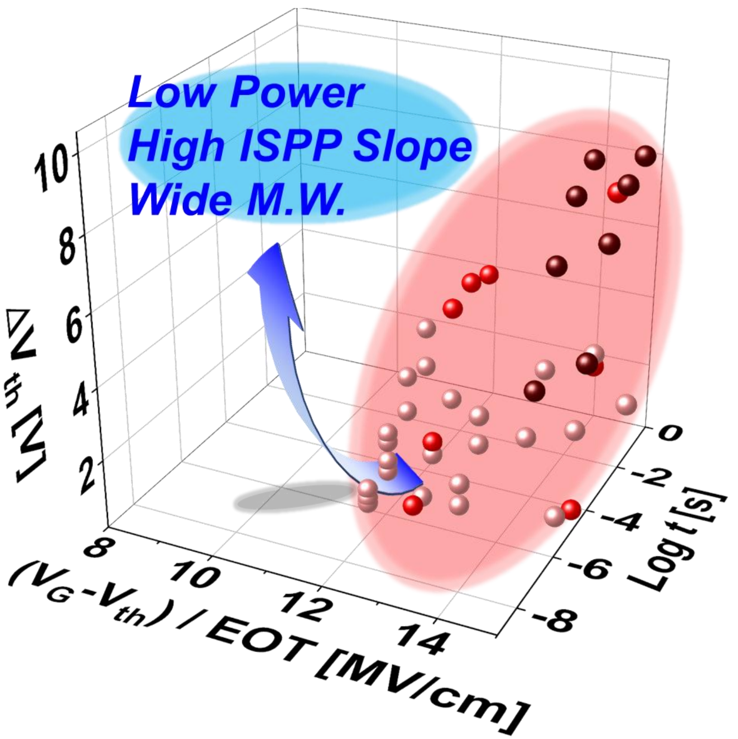

Concept of Negative Capacitance (NC)-CTF

❖ Capacitor Network in a NC-CTF and It's Simplified Model.

- **NC-CTF is demonstrated by integrating a BL in which the NC effect is stabilized.**

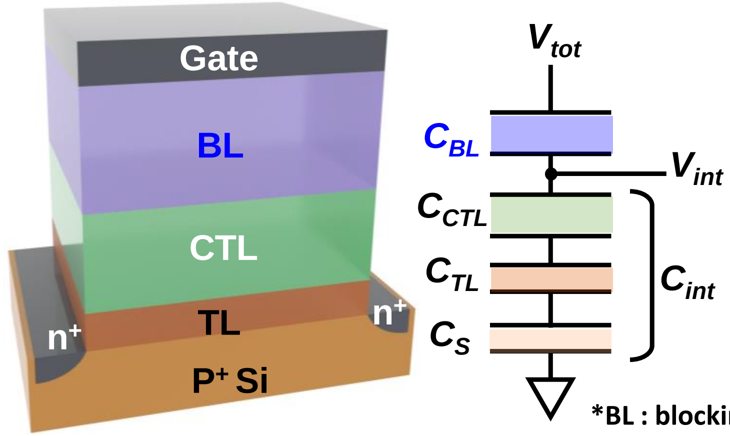

*BL : blocking layer
CTL : charge trap layer
TL : tunneling layer

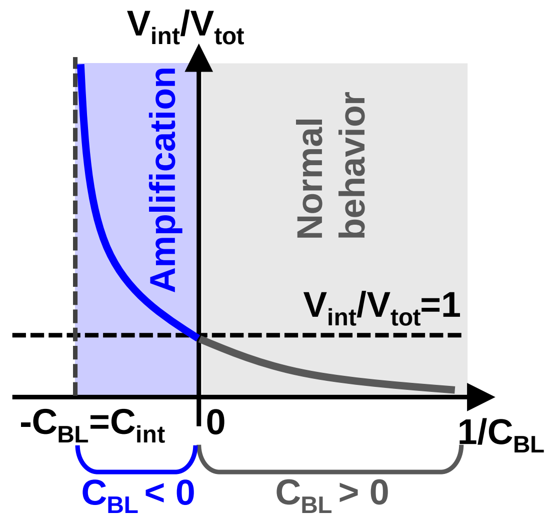

- $C_{int} = (\frac{1}{C_{CTL}} + \frac{1}{C_{TL}} + \frac{1}{C_S})^{-1}$
- $C_{tot} = (\frac{1}{C_{BL}} + \frac{1}{C_{int}})^{-1}$
- $Q = C_{tot} \cdot V_{tot} = C_{int} \cdot V_{int}$
- $\frac{V_{int}}{V_{tot}} = (1 + \frac{C_{int}}{C_{BL}})^{-1}$

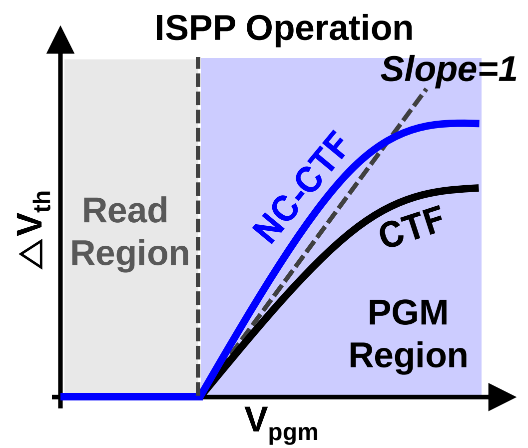

Concept of NC-CTF Device

❖ Integrating RSFE-HZO/AlO Bilayer as a Blocking Layer (BL)

- **Due to the NC effect of RSFE under $+V_{PGM}$, the energy band of RSFE is bent in the opposite direction to the $+V_{PGM}$, which induces significant band bending of the underlying layers, enhancing the electric field through the tunneling layer (TL).**

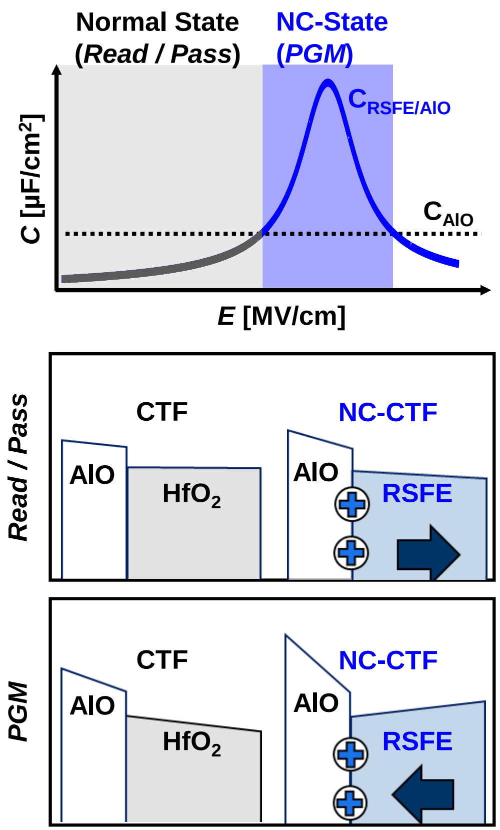

Band Diagram of Blocking Layer

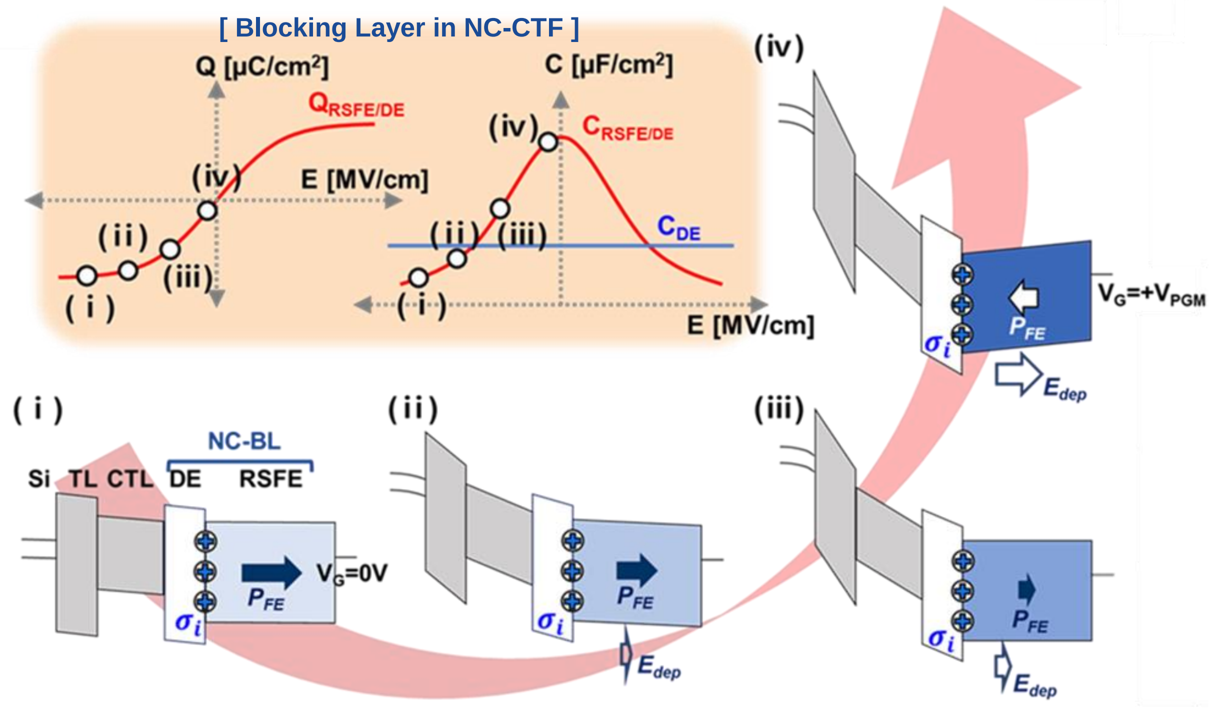

Fabrication of NC-CTFs

❖ NC-CTFs were fabricated by integrating RSFE-HZO / AlO as the BL

- **The fabricated NC-CTF device shows the basic characteristics of a typical CTF device.**

- FOX growth
- Active area patterning
- Channel doping
- Replacement gate deposition
- S/D implant
- Replacement gate removal
- S/D activation
- Standard (RCA) Cleaning
- Thermal oxidation (Tunnel oxide)
- Nitride deposition (Charge trap layer)
- AlO deposition (#1 Blocking oxide)
- HZO deposition (#2 Blocking oxide)
- HPPDA
- TiN deposition
- Gate patterning
- Metallization

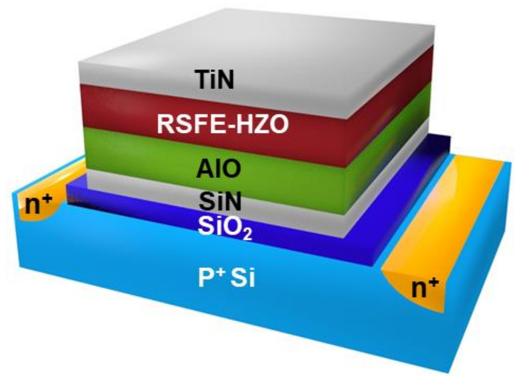

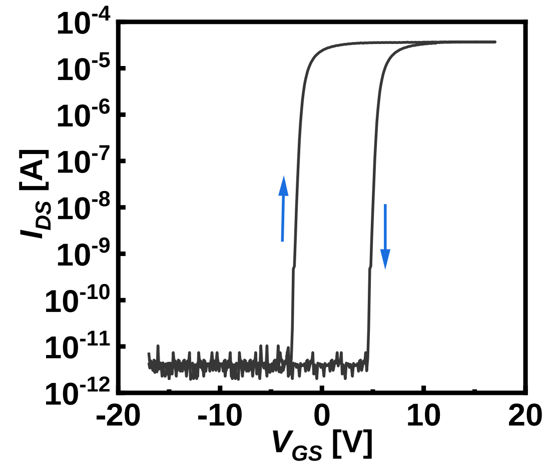

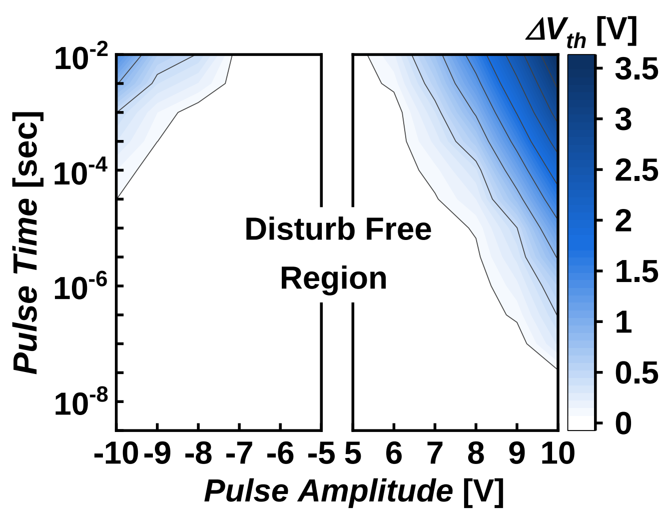

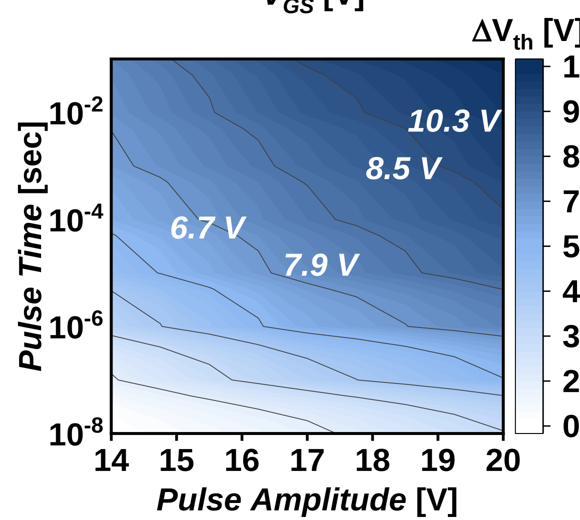

ISPP characteristics of the NC-CTF device

❖ Origins of the ISPP Mechanism of the NC-CTF Device

- **It shows that the ISPP characteristics of the NC-CTF are influenced by two mechanisms.**

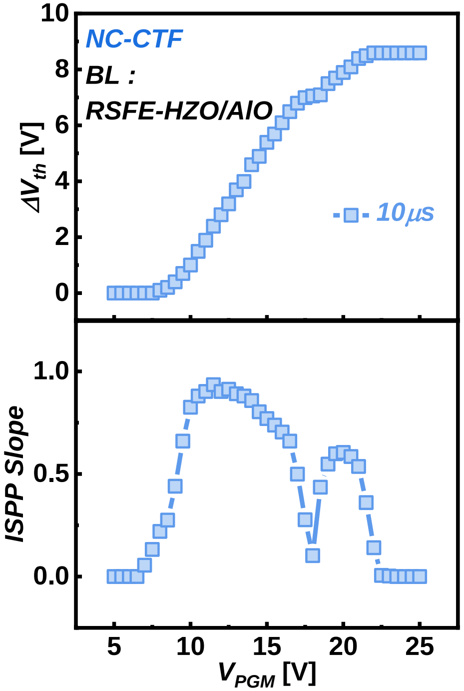

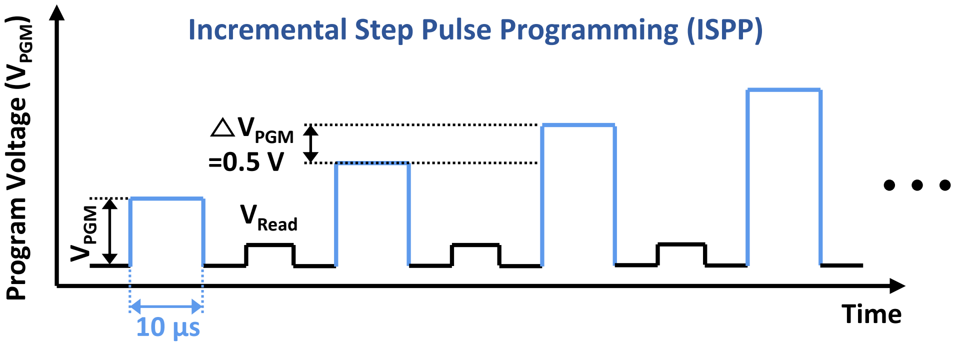

ISPP characteristics of the NC-CTF device

❖ Origins of the ISPP Mechanism of the NC-CTF Device

- **It shows that the ISPP characteristics of the NC-CTF are influenced by two mechanisms.**

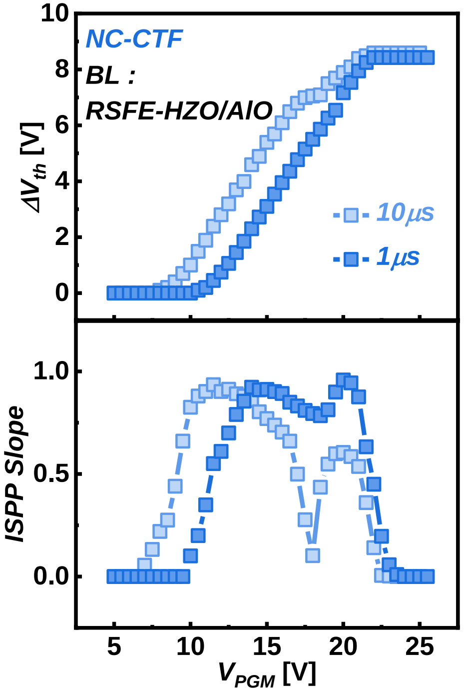

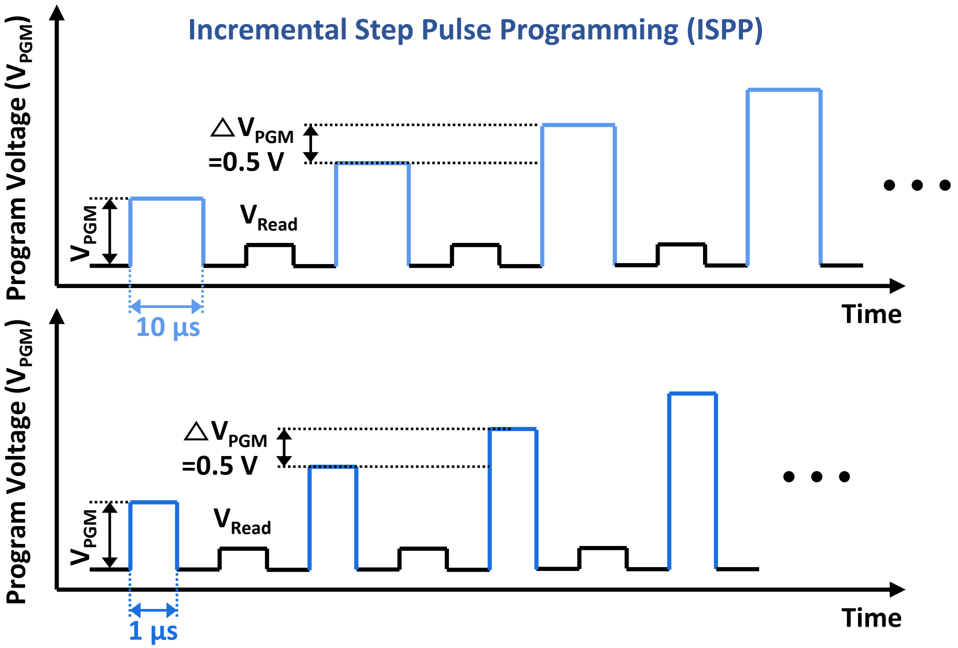

ISPP characteristics of the NC-CTF device

❖ Origins of the ISPP Mechanism of the NC-CTF Device

- **It shows that the ISPP characteristics of the NC-CTF are influenced by two mechanisms.**

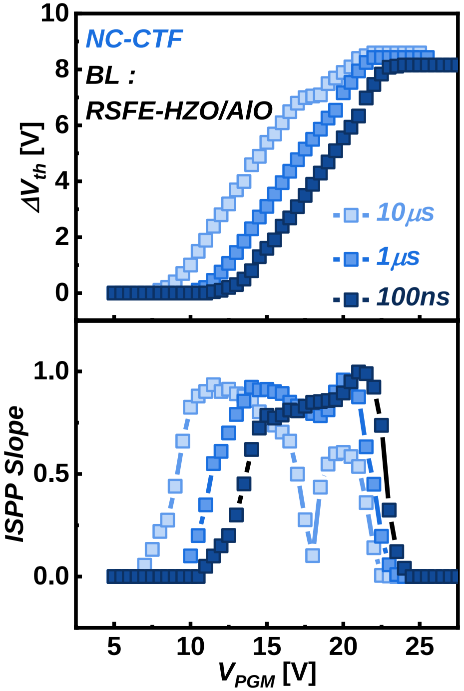

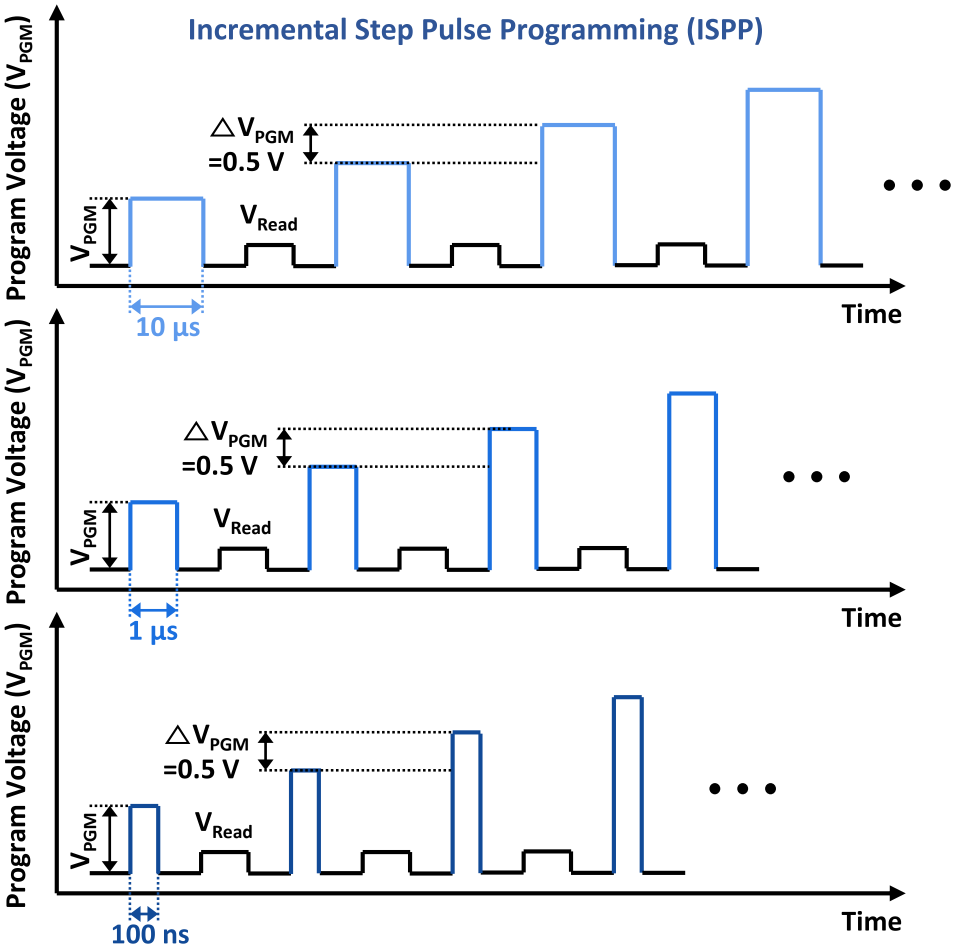

NC Effect in the NC-CTF Device

❖ Direct Experimental Evidence of the NC Effect of the RSFE-HZO/AlO BL

- **The ISPP-boosting point coincides with the NC effect of the RSFE-HZO/AlO BL.**

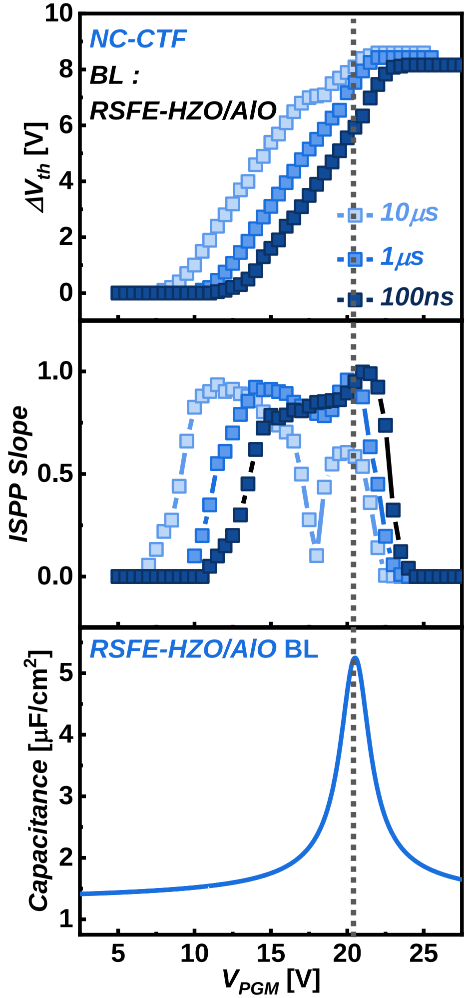

Memory switching characteristics of a CTF device

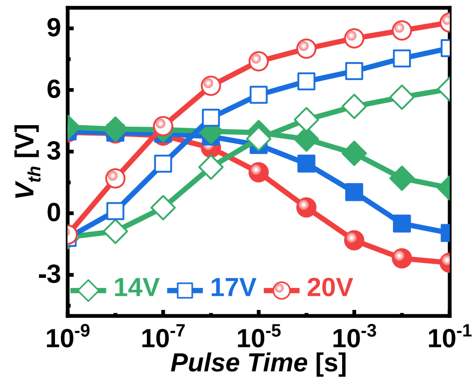

NC effect of the RSFE-HZO/AlO bilayer with various pulse time

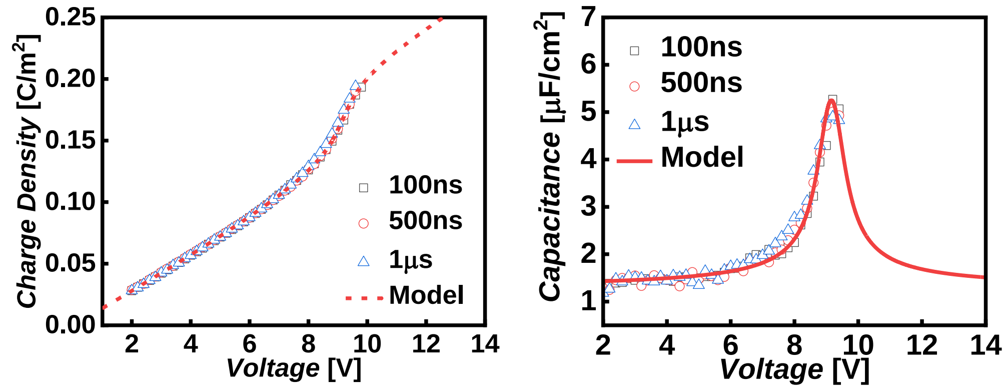

The Superior ISPP Performance of the NC-CTF

❖ Comparison of ISPP characteristics of the CTFs with various BLs

- The NC-CTF device can provide a **steep ISPP Slope (~1.1)** and **large memory window (~8.16 V)** in **100ns ISPP operation (high speed)**.

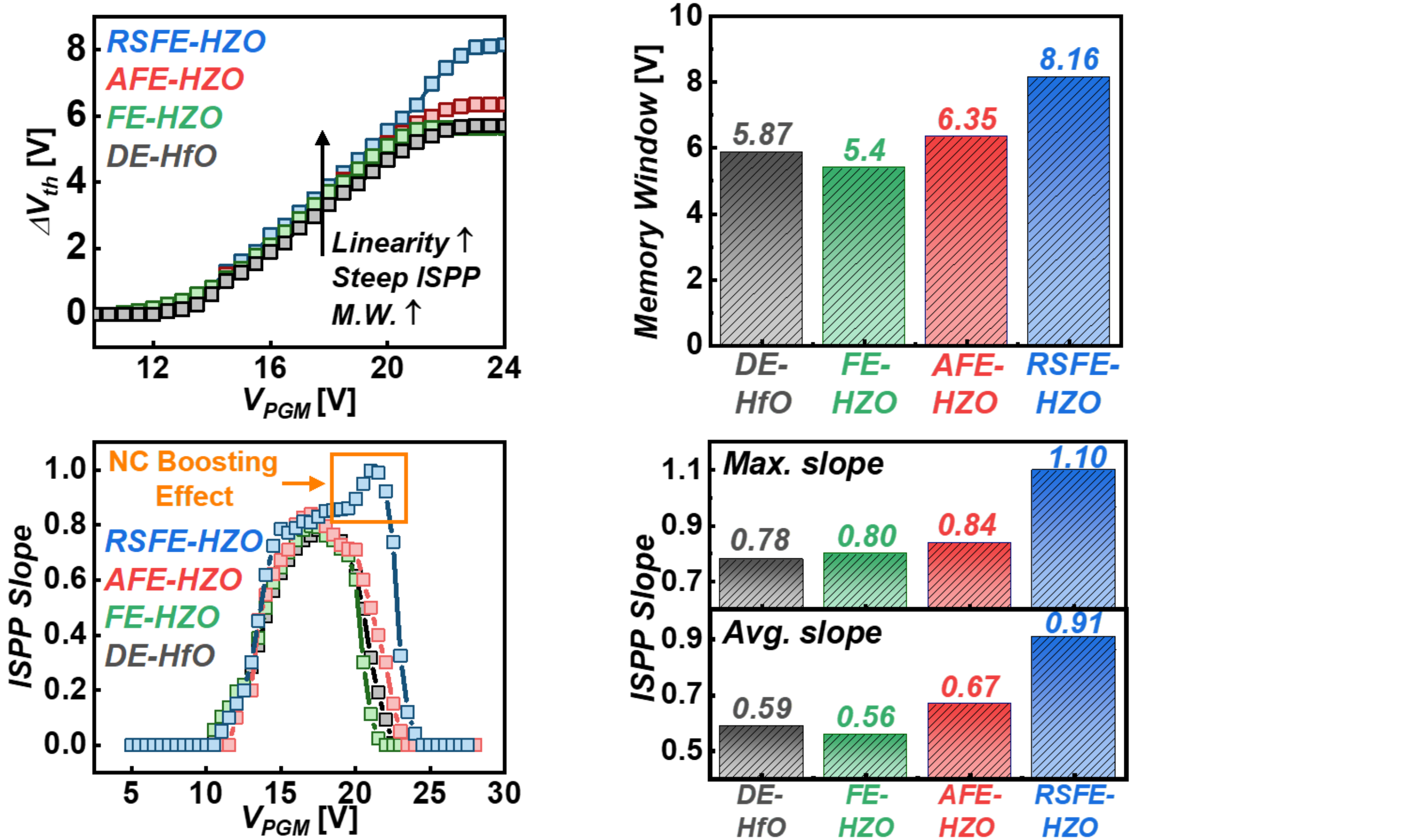

Superior Performance of the NC-CTF

❖ **The comparison was made among the proposed NC-CTF and other devices with similar structures.**

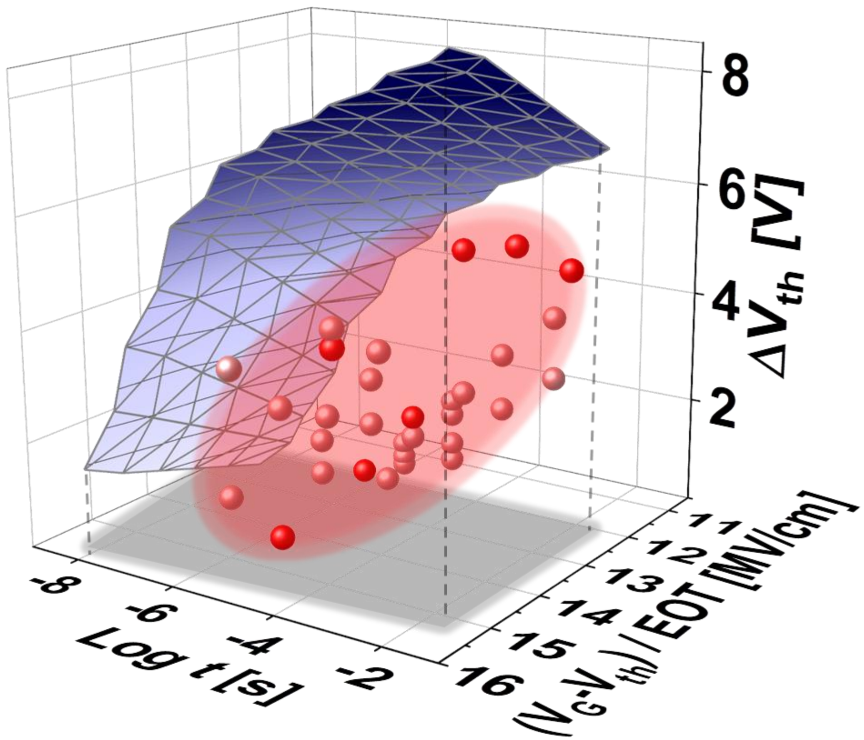

5. Application : NC-CTF Based In-Memory Computing

NC-CTF Based In-Memory Computing

❖ Local Multiply & Global Accumulate (LM-GA) Array

- **Multiply is operated in Multiply-lines (MLs) locally**
- **Accumulation is operated in Accumulate-lines (ALs) globally**

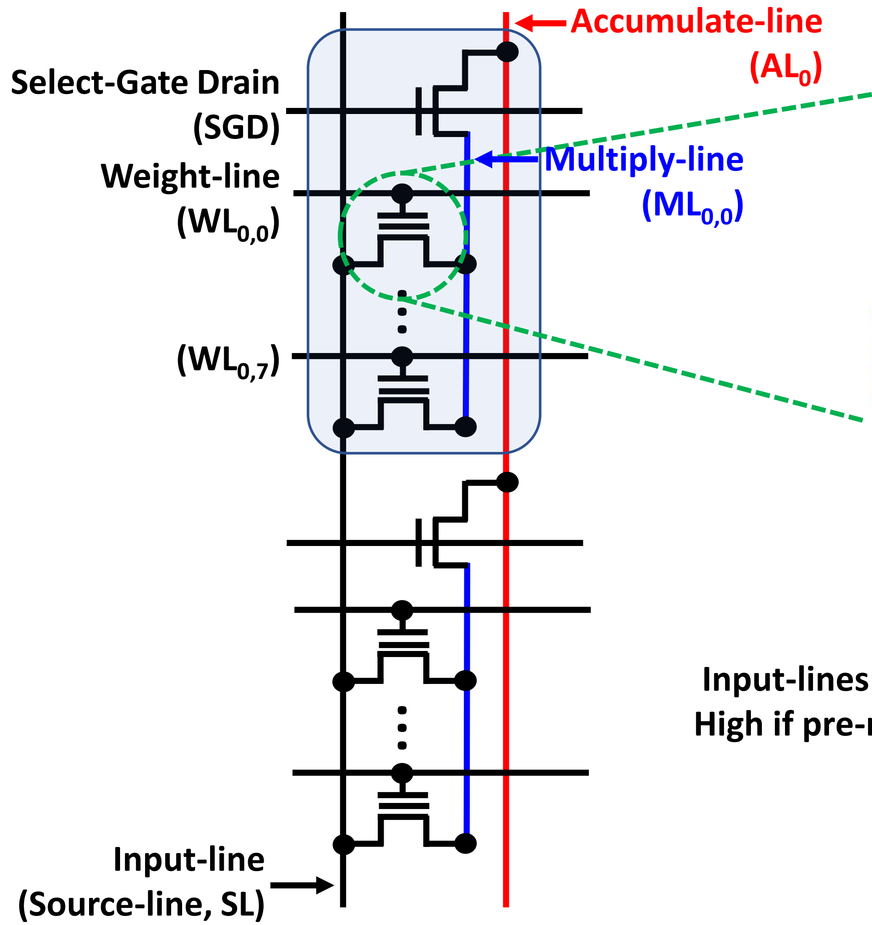

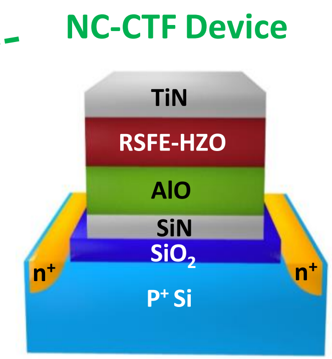

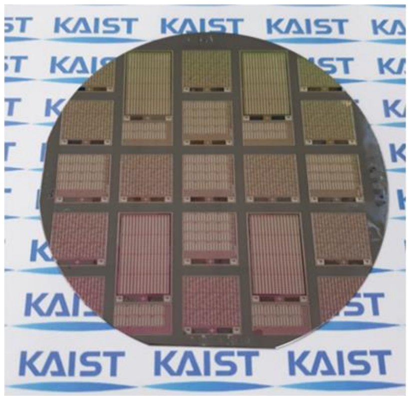

Input-lines (SLs) are High if pre-neurons fire

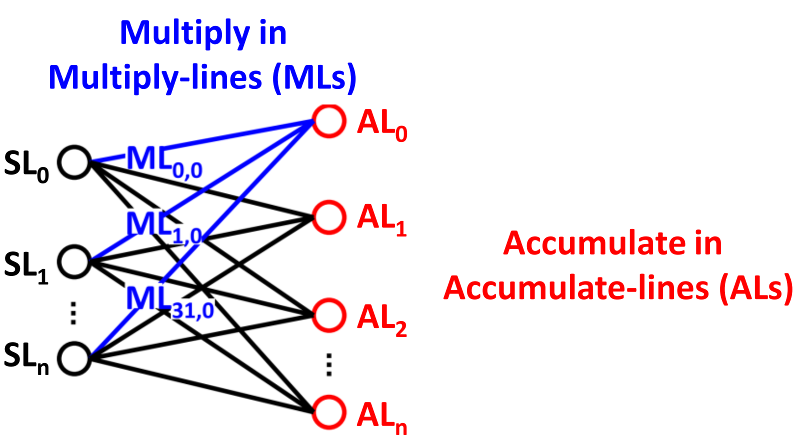

Local Multiply by Source-Follower (SF)

❖ Local MLs Multiply Input (SL) and Weights by Source-Follower (SF)

- Neural network weights are stored in NC-CTF as $V_{TH}^{(SF)}=V_G-V_{ML}$
- Read time is short because of small capacitance of local MLs

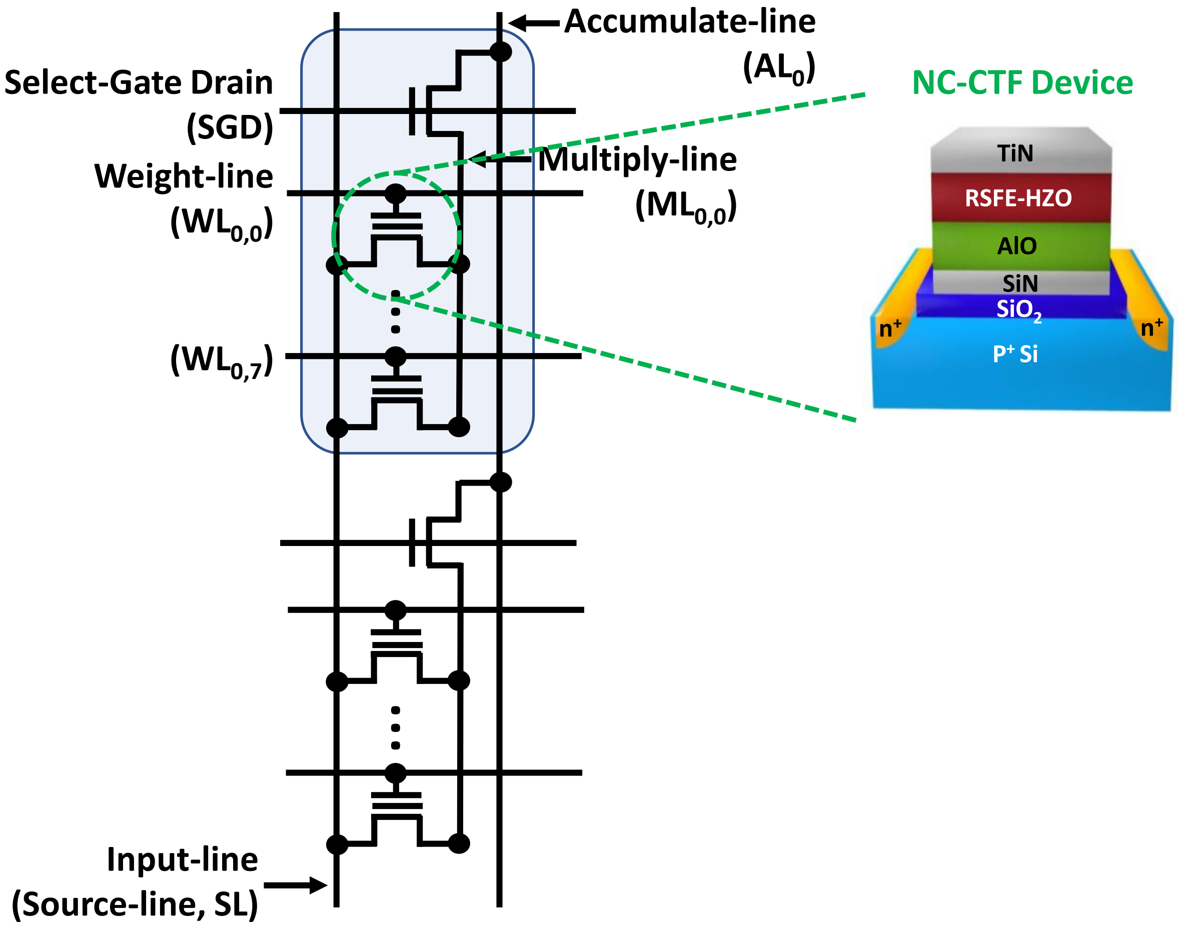

Local Multiply by Source-Follower (SF)

❖ Local MLs Multiply Input (SL) and Weights by Source-Follower (SF)

- **In the LM-GA array, the VMM operation was conducted row by row**

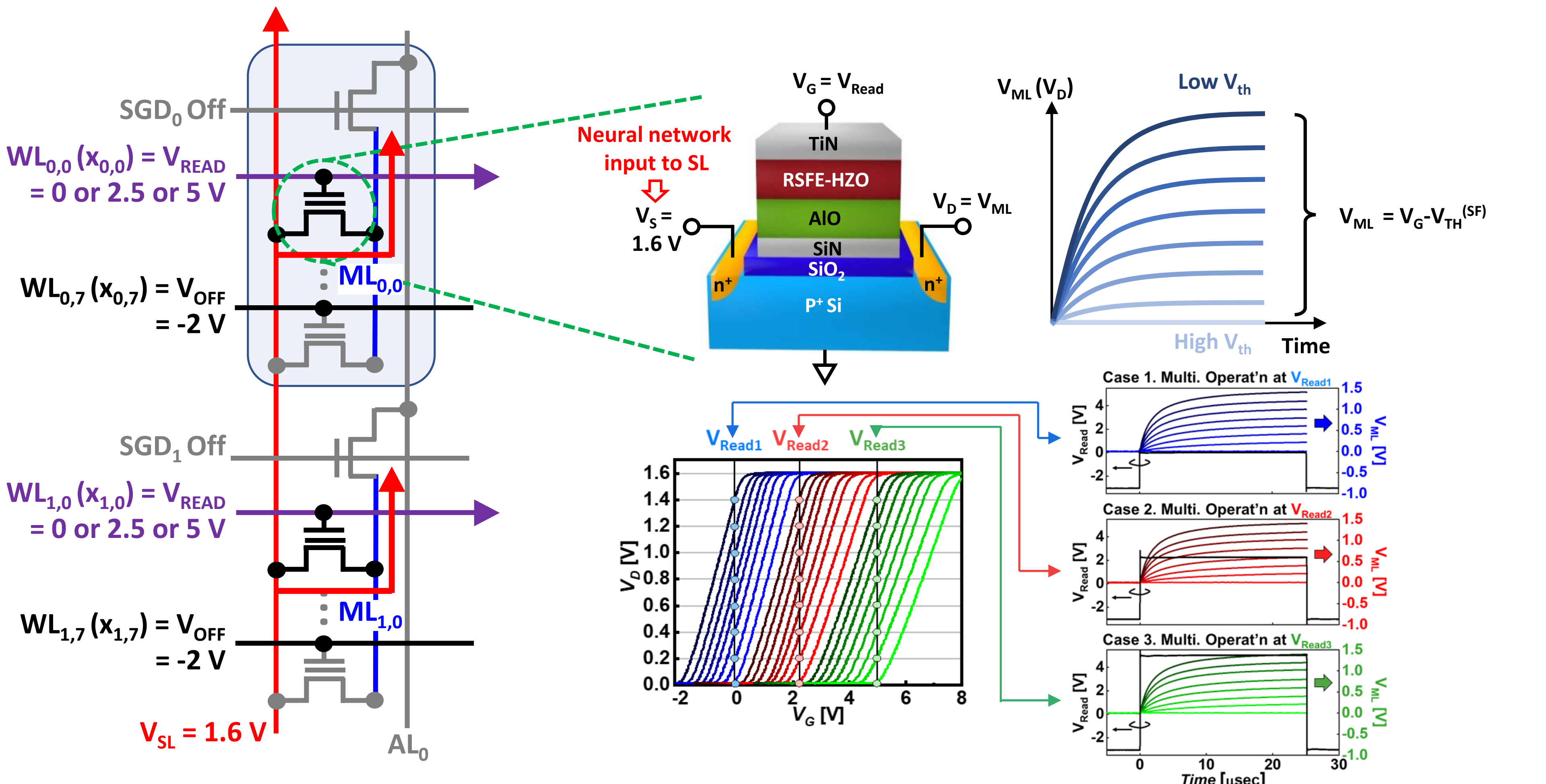

Global Accumulate by Charge-Sharing (CS)

❖ Global AL accumulates $V_{TH}^{(SF)}$ of LM-GA array by charge-sharing

- After multiplication, all NC flash devices are turned off and the MLs becomes floating
- When the SGD is turned on, the charge of each ML is transferred to the AL by charge sharing

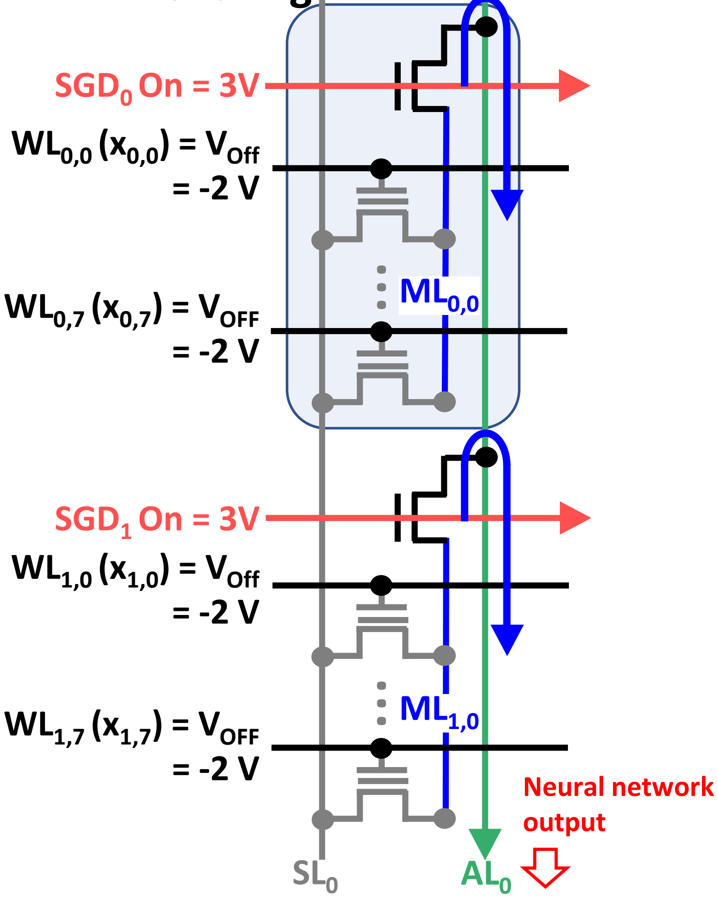

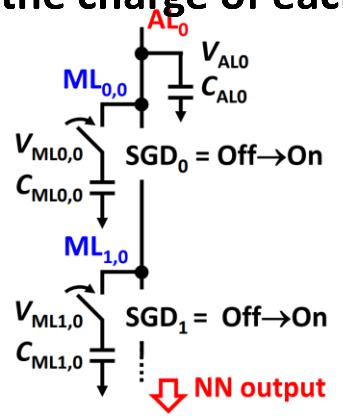

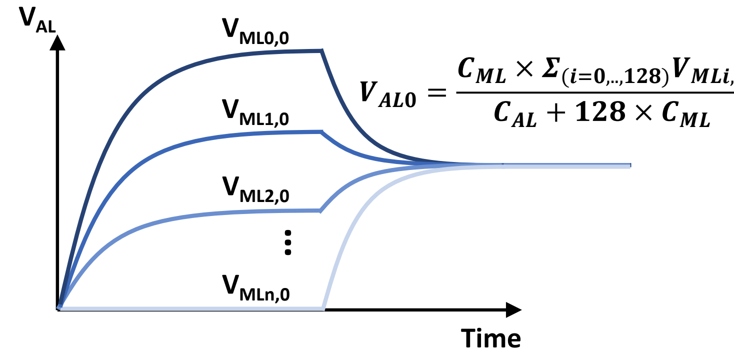

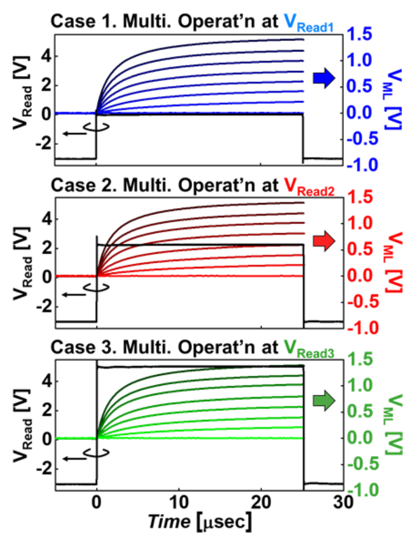

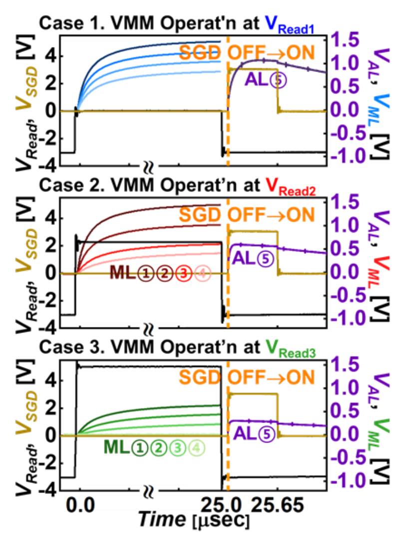

System-Level Energy Efficiency Evaluation

❖ System-Level Evaluation Using the DNN+NeuroSIM Framework

- The DNN+NeuroSIM framework based on 28 nm PTM was used.
- To reflect the proposed voltage-sensing MAC operation and local NC-CTF array structure, we modified the array structure of the DNN+NeuroSIM framework.

*PTM : Predictive technology model

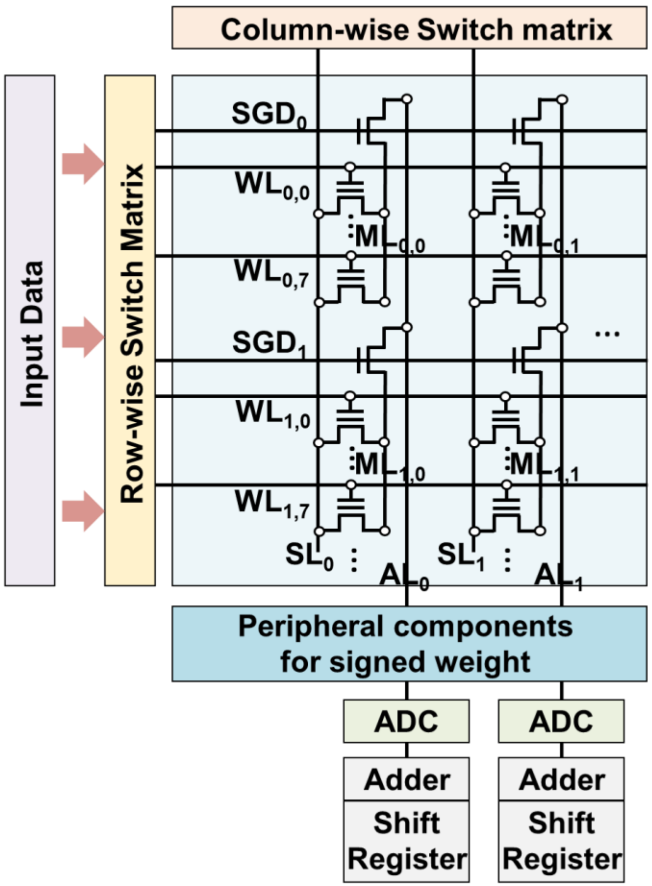

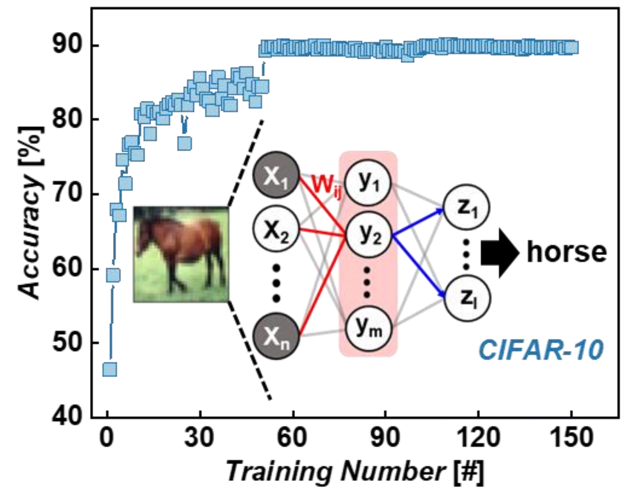

Summary & Comparison of Key Features

❖ Benchmark Table of In-Memory Computing Performance

- **The neural network using the NC-CTF based IMC exhibits excellent computational efficiency and accuracy**

	2018 ISSCC [1]	2019 ISSCC [2]	2019 ISSCC [3]	2021 VLSI [4]	In this Work
Device	SRAM	ReRAM	SRAM	FeFET	NC-CTF
Technology	65 nm	55 nm	55nm	-	28 nm
Bit/cell	1 bit	1 bit	1 bit	3 bit (Feasible)	4.58 bit
F^2/bit	130	66	-	12	7.9
Input / weight / output [bit]	8 / 8 / -	1 / 3 / 4	4/5	1 / 3 / -	1 / 4.58 / 6
Tops/W x input bit x weight bit	199.7	159.5	367.4	192	407.6
Tops/W	3.21	53.17	18.37	66	89
Accuracy	-	~ 89 %	90.42 %	-	90.02 %

Source: [1] S. Gonugondla, ISSCC (2018)
[2] C.-X. Xue, ISSCC (2019)
Source: [3] X. Si, ISSCC (2019)
[4] C. Matsui, Symposium on VLSI (2021)

Summary

Summary

- We successfully developed a CMOS-compatible (reversible domain switching ferroelectric) HZO film by applying FG-HPPDA to stabilize the NC effect.
- FG-HPPDA generates a homogeneously aligned phase and reversible domain switching by inducing both a strain gradient induced internal field (flexoelectric effect) and chemically induced surface polarization pinning (surface effect).
- The homogeneously aligned single-domain with the reversible domain switching of the RSFE-HZO film enables to induce a stable NC effect.
- An unprecedented strategy of introducing an RSFE-HZO/AlO layer with a stable NC effect as the BL of CTF memory was presented and the high-performance operation of the NC-CTF was successfully demonstrated.
- Additionally, we demonstrate energy-efficient, and high-density NC-CTF IMC

Thank you